

Multi-approach study of *Pla2g4e* involvement in obesity development in unique fat and lean mouse lines

Maša Čater¹, Nejc Umek², Efua Gyakyew Ewusi-Brown², Erika Cvetko², Urška Hostnik¹, Špela Mikec¹, Martin Šimon¹, Nicholas Morton³, Tanja Kunej¹, Simon Horvat¹

¹University of Ljubljana, Biotechnical Faculty, Department of Animal Science, Chair of Genetics, Animal Biotechnology and Immunology, Domžale, Slovenia

²University of Ljubljana, Faculty of Medicine, Institute of Anatomy, Ljubljana, Slovenia

³University of Edinburgh, The Queen's Medical Research Institute, Centre for Cardiovascular Science, Edinburgh, United Kingdom

INTRODUCTION

Obesity is controlled by a combined effect of genetic and environmental factors. The mechanisms of action that trigger metabolic disorders have not been fully discovered yet.

In our study, we used the Fat (F) and Lean (L) mouse lines representing unique polygenic models of obesity and leanness (Fig. 1). Previous transcriptome studies on these lines fed standard maintenance chow diet identified gene *Pla2g4e* as differentially expressed in hypothalamus and muscle tissue. *Pla2g4e* is involved in nutrient metabolism and energy expenditure. It is highly expressed in the skeletal muscles and is involved in their metabolism and function.

Our experiment aimed to study *Pla2g4e* on RNA and protein levels comparing F and L mouse lines.

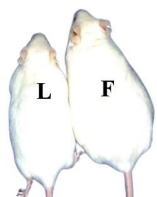


Fig. 1: Our unique mouse models for studying leanness and obesity. L - Lean line, F - Fat line.

METHODS

Mice of F and L lines of both sexes were fed two different isocaloric diets from weaning to the age of 14 weeks:

- high-fat diet (HFD) or
- low-fat diet (LFD)

Mouse body weight and feed intake were monitored weekly.

Mice were sacrificed at the age of 14 weeks and skeletal muscle tissue was collected and frozen at -80 °C.

Musculus gastrocnemius:

- RNA isolation
- *Pla2g4e* mRNA expression analysis by quantitative real-time PCR method (house-keeping genes *Gapdh* and *Actb*)

M. gastrocnemius, *m. soleus*, *m. tibialis anterior*:

- fluorescent immunostaining of cPLA ϵ , the protein product of *Pla2g4e* (anti-Pla + ARF/ART)
- differential DAB-immunostaining of different muscle fibers (SC71/BFF3 + P260)
- muscle fiber type-related cPLA ϵ expression analysis with Ellipse software

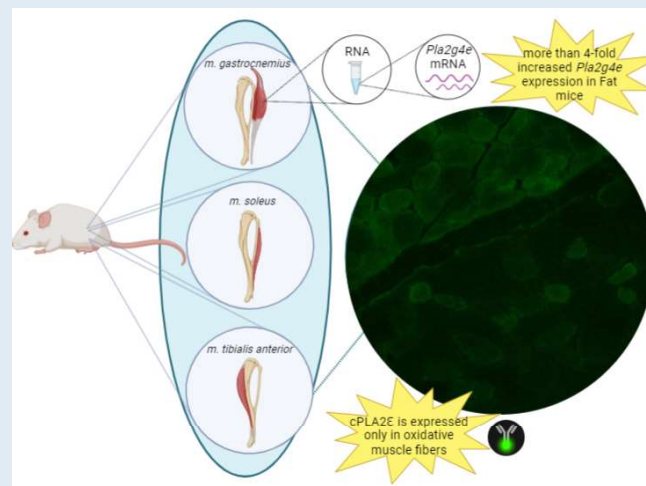
Bioinformatic analyses for determining CTCF and miRNA-binding sites and genome organization:

- TargetScan
- CTCFSDDB database

Obesity in Fat mice developed despite the same feed intake as Lean mice and regardless of the diet type.

Pla2g4e product, cPLA ϵ , is synthesized only in oxidative muscle fibers (I and IIa).

Pla2g4e is overexpressed in skeletal muscles of Fat mice of both sexes. Polymorphisms in regulatory regions of Fat line may be affecting rate of transcription, miRNA silencing or RNA stability, leading to difference in protein expression. This results in **altered muscle aerobic respiration** that may contribute to obesity development.



CONCLUSION

These results point to the importance of genetic background in obesity development and suggest that *Pla2g4e* is one of the potential novel genetic factors highly linked to obesity that deserves further functional and mechanistic research.

RESULTS

BODY WEIGHT

Diet type affected body weight of mice. Mice on HFD were heavier than mice on LFD. The effect of genetic background on body weight was significant, as male and female mice of the Fat line were heavier than male and female mice of the Lean line (Figure 2), regardless of the diet type. Interestingly, their feed intake was the same.

Pla2g4e EXPRESSION IN SKELETAL MUSCLE

The expression of *Pla2g4e* in *m. gastrocnemius* in Fat mice was several times higher than in Lean mice (Figure 3), regardless of the diet. A significant *Pla2g4e* fold change can be seen in both males and females.

cPLA ϵ EXPRESSION PATTERN IN SKELETAL MUSCLE

cPLA ϵ expression was determined immunohistochemically in type I (slow oxidative) and IIa (fast oxidative) fibers of skeletal muscles, which were present in small quantity in *m. gastrocnemius* and *tibialis anterior* and in greater quantity in *m. soleus* (Figure 4).

Effect of genetic background and diet on body weight

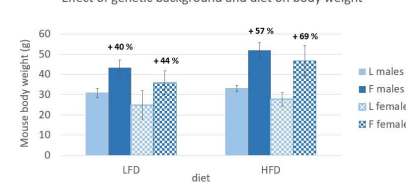


Figure 2: Mice of both sexes from the Fat line were heavier than mice from the Lean line in both diet treatments.

Fat vs. Lean mouse line
m. gastrocnemius Pla2g4e expression

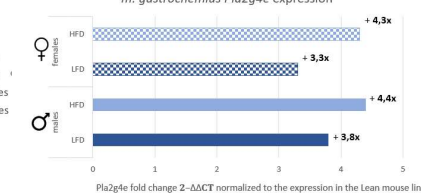


Figure 3: Expression of *Pla2g4e* in *m. gastrocnemius* represented as a fold change when comparing the Fat mouse line to the Lean mouse line.

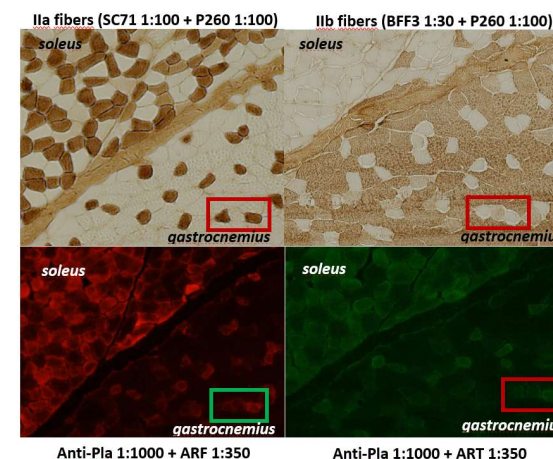


Figure 4: A zoomed section of interconnected *m. soleus* and *m. gastrocnemius* skeletal muscles of a control mouse after differential DAB-immunostaining for IIa and IIb muscle fibers (brown signal) and fluorescent immunostaining for cPLA ϵ (ARF-red or ART-green signal).

BIOINFORMATIC ANALYSIS OF *Pla2g4e* REGION

Many miRNAs are predicted to be involved in post-transcriptional modifications of *Pla2g4e*. Genetic variants within predicted miRNA target sites in 3'UTR and CTCF binding motifs in the intronic region of *Pla2g4e* were found in Fat, but not in Lean mice → possible protection in Fat mice from various silencing mechanisms resulting in an increased expression of *Pla2g4e* and therefore, in modified metabolism associated with obesity development.

Immunohistochemical results from Fat and Lean mice are still under analysis. Are there differences in cPLA ϵ expression in skeletal muscle between the mouse lines or between sexes? Could differential cPLA ϵ expression in muscle fibers be one of the causes for the development of metabolic syndrome and obesity in Fat line mice?

SARS-CoV-2 cell entry and its inhibition using short antioxidant peptides

Tea Govednik^{1,2}, Duško Lainšček^{1,3}, Urška Kuhar⁴, Marva Lachish⁵, Sandra Janežič⁶, Malan Štrbenc⁷, Uroš Krapež⁸, Roman Jerala^{1,3}, Daphne Atlas⁵, Mateja Manček-Keber^{1,3}

¹ Department of Synthetic Biology and Immunology, National Institute of Chemistry, Ljubljana, Slovenia; ² Graduate School of Biomedicine, University of Ljubljana, Ljubljana, Slovenia; ³ Centre of Excellence EN-FIST, Ljubljana, Slovenia; ⁴ Institute for microbiology and parasitology, Veterinary Faculty, University of Ljubljana, Ljubljana, Slovenia; ⁵ Hebrew University of Jerusalem, Jerusalem, Israel; ⁶ National Laboratory of Health, Environment and Food, Maribor, Slovenia; ⁷ Institute for preclinical sciences, Veterinary Faculty, University of Ljubljana, Ljubljana, Slovenia; ⁸ Institute of poultry, birds, small mammals and reptiles, Veterinary Faculty, University of Ljubljana, Ljubljana, Slovenia

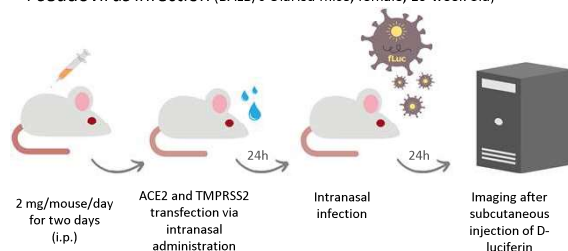


BACKGROUND

Spike protein is a homotrimer; each protomer is rich in cysteine residues, and many form disulfide bonds. Disulfide bonds are essential for protein structure, and their integrity is also necessary for spike binding to the ACE2 and viral entry into host cells^{1,2}. Thioredoxin mimetic (TXM) peptides were designed to mimic thioredoxin activity, therefore containing its typical active motif that facilitates redox reactions. TXM peptides comprise two cysteine residues flanking either one or two amino acids, and by mimicking thioredoxin activity, these peptides represent a platform of intracellular reducing molecules³. **Our study aimed to test the viral entry inhibitory potential of TXM peptides and examine their anti-inflammatory activity.**

METHODS in vivo

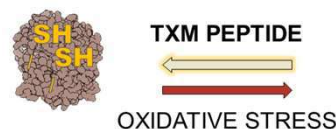
- Pseudovirus infection (BALB/c OlaHsd mice, female, 10-week old)



The animal study was performed according to the directives of the EU 2010/63 and was approved by the AFSVSP, Republic of Slovenia. All animals used in the study were healthy and accompanied by health certificates from the animal vendor. Mice were housed in IVC cages (Techniplast) and maintained in a 12-12 dark-light cycle. Animals were fed standard chow (Mucedola) and provided with tap water ad libitum.

- Anti-inflammatory study (BALB/c)

Mice were challenged with intratracheal instillation of LPS, then the anti-inflammatory activity of TXM-CB3 was determined. The compound was injected intravenously at three time points (15min prior, 24h after, and 48h after LPS). The effect of LPS-induced inflammatory damage was examined by the differential cell count in Broncho alveolar lavage fluid (BAL) by flow cytometry. Levels of cytokines in BAL fluid were measured by ELISA. Experiments were performed by Science in Action, Ltd; Ness-Ziona, Israel. All animals were treated according to the National Institute of Health (NIH) guidelines for the care and use of laboratory animals.



- As shown with ELISA and sensitive split reporter cell assays, TXM peptides **inhibited SARS-CoV-2 spike protein binding** to the ACE2 receptor and **syncytia formation** in a dose-dependent manner.
- In addition to inhibition of **pseudovirus** cell infection, thiol-reducing compounds also prevented **Wuhan, Alpha, Delta and Omicron viral infection** and replication in cells.
- **TXM peptides antioxidant activity** was determined by reversal of the oxidative stress-induced phosphorylation of the MAPK's ERK1/2 and JNK1/2.
- Several TXM peptides inhibited **pseudovirus infection in vivo**, further confirming the efficiency and potential of thiol-reducing compounds as antiviral therapeutic (Figure 1).

- **TXM-CB3 mitigated LPS-induced inflammation in vivo.**

The significant increase in neutrophils and eosinophils induced by LPS in BAL of LPS-treated mice was lowered by TXM-CB3. Cytokine levels were also significantly decreased, where the tested compound lowered the LPS-induced IFN- γ , IL-2, and CXCL10 (Figure 2).

RESULTS in vivo

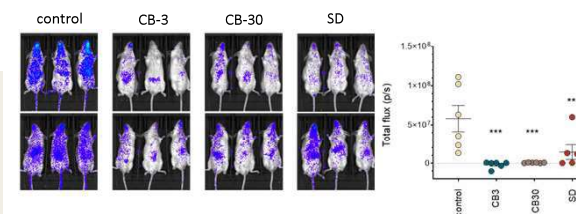


Figure 1. Thiol based peptides mitigate pseudovirus infection in vivo.

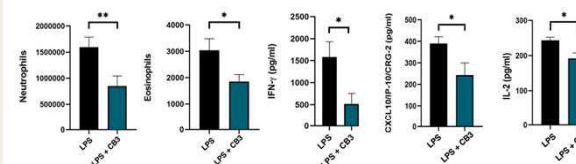


Figure 2. TXM-CB3 lowers LPS-induced neutrophils, eosinophils and cytokines in BAL.

CONCLUSIONS

Thiol-reducing peptides based on the active site of oxidoreductase thioredoxin (TXM peptides) are able to prevent SARS-CoV-2-related syncytia formation, viral entry and replication in cells and infection in a mouse model. Furthermore, TXM peptides lower inflammation in mice, thus exerting anti-inflammatory properties. **Due to their redox properties and anti-inflammatory activity, TXM peptides may prove beneficial in treating COVID-19 and related post-infection symptoms.**



¹Grishin, A. M. et al. *J. Mol. Biol.*, 434(2), p. 167357 (2022).

²Lan, J. et al. *Nature*, 581(7807), pp. 215–220 (2020).

³Bachnoff, N., Trus, M. and Atlas, D. *Free Rad. Biol. and Med.*, 50(10), pp. 1355–1367 (2011).

Z/113. The Effect of surgical treatment of brachycephalic obstructive airway syndrome on thermoregulatory response to exercise in French bulldogs

Žiga Žgank¹, Alenka Nemec Svete¹, Helena Lenasi², Janez Vodičar³, Erjavec Vladimira¹

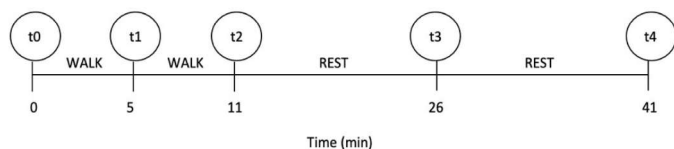
¹Small Animal Clinic, Veterinary Faculty, University of Ljubljana, Slovenia, ²Institute of Physiology, Faculty of Medicine, University of Ljubljana, Slovenia, ³Institute of Sport, Faculty of Sports, University of Ljubljana, Slovenia

BACKGROUND

- Brachycephalic dogs are predisposed to respiratory and thermoregulatory problems.
- This is referred as Brachycephalic Obstructive Airway Syndrome (BOAS).
- They are 2.1 times more susceptible to heat-related injuries at low ambient temperatures and relatively low levels of physical activity.
- Surgical treatment alleviates clinical signs, potentially improving thermoregulatory ability of the dogs with BOAS.
- Aim: to investigate the thermoregulatory response in French bulldogs with BOAS.

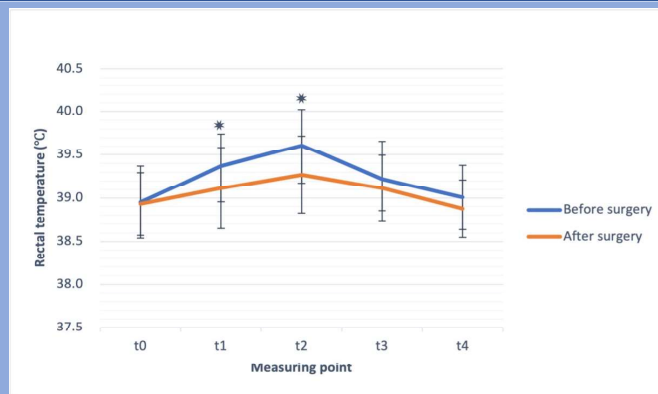
METHODS

- 13 privately owned French bulldogs.
- Dynamic exercise on a treadmill.
- Rectal temperature (RT) and heart rate (HR) were assessed.
- 2 independent sessions (before, after surgery).
- 2 consecutive 5-minute walks at 2.5 km/h and inclination of 0% and 5%, 30-min recovery.

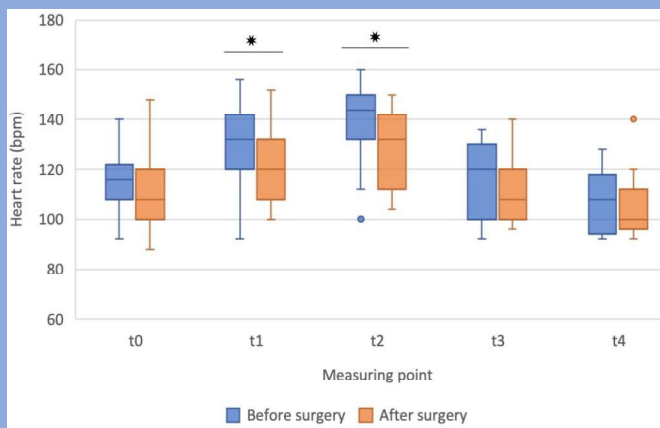


The timeline of the testing protocol; t0-t4 indicating the measuring points of the RT and HR.

RESULTS



Rectal temperature before exercise (t0), during exercise test (t1, t2) and in the recovery (t3, t4), *p < 0.05, paired sample t-test.



Heart rate before (t0), during exercise (t1, t2) and in the recovery (t3, t4) before the and after the surgery, *p < 0.05, Wilcoxon signed-rank test.

RESULTS

- Lower increase of RT after the surgery (at t1 p = 0.004; at t2 p < 0.001) than before the surgery.
- Lower RT at the end of the exercise test (p = 0.033) after the surgery compared to before the surgery.
- Lower HR during exercise at t1 (p = 0.020) and at t2 (p = 0.011) after the surgery than before the surgery.
- The increase of RT and HR correlated before and after the surgery.

CONCLUSION

- Surgical treatment of BOAS can improve the thermoregulatory response to exercise in French bulldogs with BOAS.
- Surgery remains the treatment of choice for affected dogs and should be advised to owners of the dogs with BOAS.

ACKNOWLEDGEMENTS

- The authors thank the dog owners for including their dogs in the study.
- This research was funded by the Slovenian Research Agency (ARRS); program No. P4-0053.



Molecular marker WUR10000125 associated with genetic resistance to PRRSV infection



Sanja Bogičević¹, Suzana Krhlanko¹, Anita Ule,¹ Andrej Kastelic,² Milena Kovač¹, Špela Malovrh¹

¹ University of Ljubljana, Biotechnical faculty, Department of Animal Science, Groblje 3, 1230 Domžale, Slovenia

² Institute of Agriculture and Forestry Novo mesto, Šmihelska cesta 14, 8000 Novo mesto, Slovenia

INTRODUCTION

Porcine reproductive and respiratory syndrome (PRRS) is characterised by reproductive disorders in sows and respiratory disease in pigs of all ages, resulting in enormous economic losses, as well as compromising animal welfare.

AIMS

- Determine the frequency of alleles A and G and genotypes AA, AG and GG in Slovenian pig populations.
- Determine if selection affects the frequency of allele G.

MATERIALS AND METHODS

Samples

- Ear tissue from 2068 pigs

SNP genotyping

- The Gene-Seek Neogen Genomic Profiler Porcine (GGP)
- Genotyping results for the GBP1 gene associated with tolerance to PRRSV (SNP WUR10000125 A>G)

Statistical analysis

Statistical analysis was performed with a SAS 9.4 statistical program using procedure proc freq for non-parametric χ^2 Test.

RESULTS

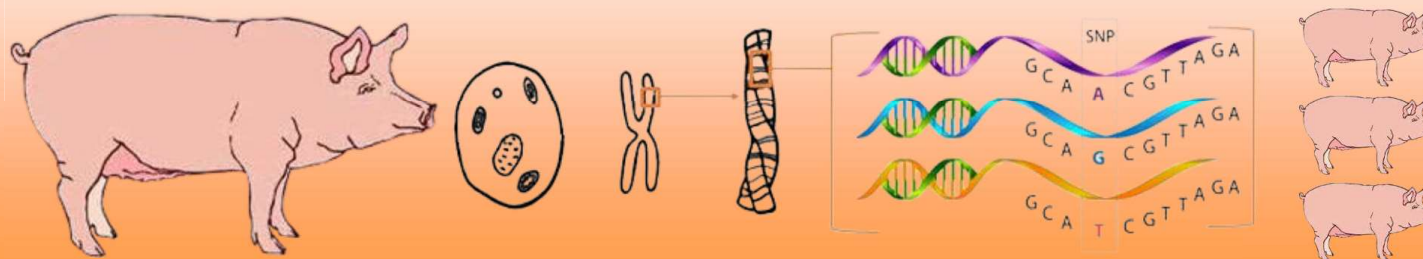
Breed	AA		AG		GG		Allele Frequency		p-value
	No	%	No	%	No	%	A	G	
11	253	74.4	87	25.6	0	0.0	87.2	12.8	0.0040
22	21	87.5	3	12.5	0	0.0	93.8	6.3	1.0000
33	20	95.2	1	4.8	0	0.0	97.6	2.4	1.0000
44	220	80.3	52	19.0	2	0.7	89.8	10.2	0.7520
55	131	97.0	4	3.0	0	0.0	98.5	1.5	1.0000
88	1268	75.8	381	22.8	41	2.5	87.2	13.9	0.0610
12	34	97.1	1	2.9	0	0.0	98.6	1.4	1.0000
43	7	100.0	0	0.0	0	0.0	100.0	0	1.0000
54	39	68.4	17	29.8	1	1.8	83.3	16.7	0.6256
1244	23	79.3	6	20.7	0	0.0	89.6	10.4	1.0000

CONCLUSIONS

- Regarding the WUR10000125 genotype, populations were in Hardy-Weinberg equilibrium except in Slovenian Landrace.
- The frequency of the G allele was higher in the local Krškopolje pig breed compared to the commercial breed.
- According to the literature, local breeds adapting to harsh environmental conditions could have increased the frequency of disease resistance alleles.

ACKNOWLEDGMENTS

This research was funded by EIP project: Sledljivost porekla pri pasmi krškopoljski prašič (3011/2018/11)



Vitamin A supplementation supports urothelial regeneration in a mouse model of acute nonbacterial cystitis

B. Dragar¹, S. Kranjc Brezar², T. Jesenko², M. Čemažar², R. Romih¹, D. Zupančič¹

¹ Institute of Cell Biology, Faculty of Medicine, University of Ljubljana

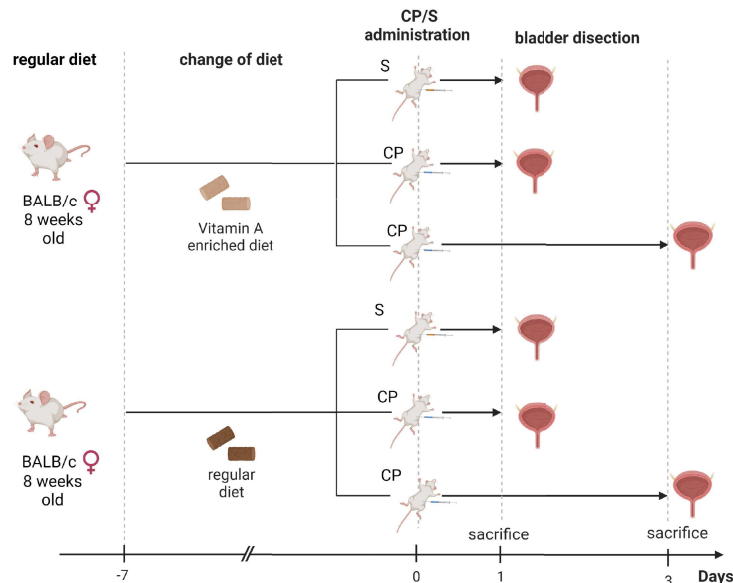
² Department of Experimental Oncology, Institute of Oncology Ljubljana

INTRODUCTION

Vitamin A or retinoids are a group of hydrophobic substances that mainly affect cell proliferation, differentiation and apoptosis. They also **possess anti-inflammatory properties**. Therefore, retinoids are used in the **treatment of various cancers and non-cancerous diseases**.

However, their **potential use** in the treatment of cystitis **has not been adequately explored**. In acute nonbacterial cystitis, the urothelium is damaged and the bladder wall is inflamed. In this case, the disruption of the urothelium is caused by chemical or physical injury. The undamaged urothelium forms a tight blood-urine barrier, which must be rapidly restored after disruption. **The aim of our study was to investigate the effects of a vitamin A enriched diet on the regeneration of the urinary bladder urothelium** in a mouse model of acute nonbacterial cystitis.

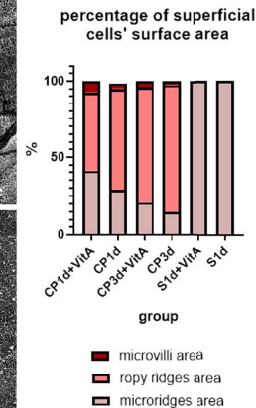
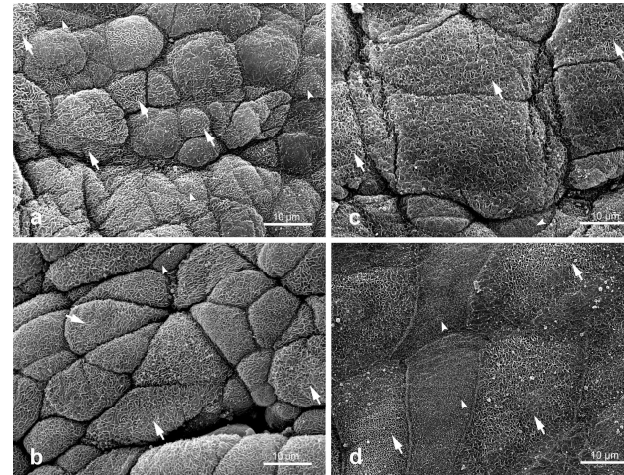
METHODS



Eighteen female BALB/c mice (8 weeks old) were used for the experiment. There were 3 mice in each group. The vitamin A-enriched diet contained 586081 UI retinyl-acetate per kilogram of diet. Cyclophosphamide was administered by intraperitoneal (i.p.) injection at a concentration of **150 mg/kg** of body weight. Urinary bladders were collected and prepared for paraffin embedding, **hematoxylin-eosin staining (HE)**, and **scanning electron microscopy**. CP - cyclophosphamide; S - saline; VitA - Vitamin A

The experiments were approved by the Ministry of Agriculture, Forestry and Food of the Republic of Slovenia (permission no. U34401-4/2022/10).

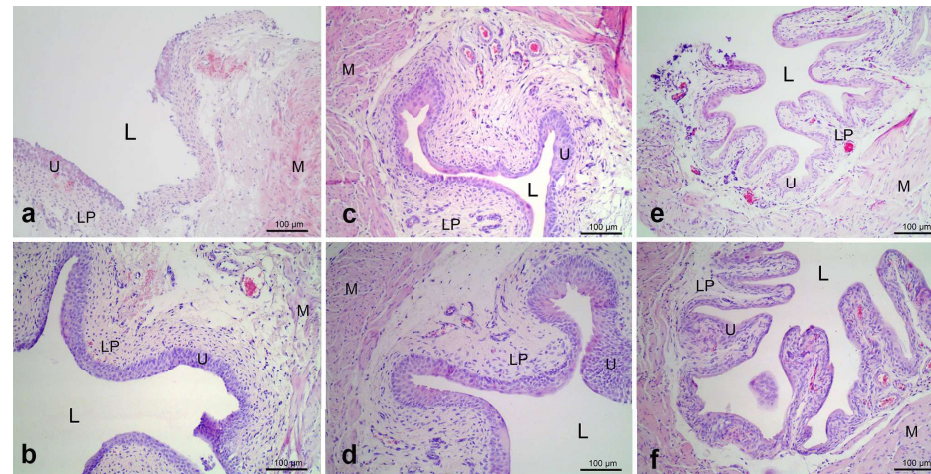
RESULTS



A higher degree of differentiation of the urothelial surface in mice fed a vitamin A-enriched diet compared with control animals fed a regular diet was determined after analysis of scanning electron micrographs (a: CP1d; b: CP1d+VitA; c: CP3d; d: CP3d+VitA).

CP1d-1 day after CP administration,
VitA-Vitamin A-enriched diet,
CP3d-3 days after CP administration;
S1d-1 day after S administration.

Arrows- ropy ridges,
arrowheads - microvilli.



HE stained mouse bladder tissue for all groups in our experiment (a: CP1d, b: CP1d+VitA, c: CP3d; d: CP3d+VitA; e: S1d; f: S1d+VitA). On these tissue sections we observed destruction of the urothelium and inflammation of the lamina propria in mice treated with CP, regardless of diet.

L = lumen,
LP = lamina propria,
U = urothelium,
M = detrusor muscle.

CONCLUSIONS

Conclusion 1: Vitamin A-enriched diet does not reduce the extent of urothelial surface damage.

Conclusion 2: Higher intake of Vitamin A could lead to slower desquamation and faster differentiation of the superficial urothelial cells.

ACKNOWLEDGEMENTS

The authors gratefully acknowledge financial support from the Slovenian Research Agency ARRS grant number P3-0108.

A big thank you to all co-workers at Institute of Cell Biology (UL MF) and Department of Experimental Oncology (Institute of Oncology Ljubljana).

The development of a four-point transversus abdominis plane block technique in pigs from an anatomical point of view

Jana Brankovič¹, Jerneja Sredenšek², Urša Lampreht Tratar³, Maja Čemažar³, Mihajlo Đokić⁴, and Alenka Seliškar²

¹Institute of Preclinical Sciences, Veterinary Faculty, University of Ljubljana, Ljubljana, Slovenia

²Small Animal Clinic, Veterinary Faculty, University of Ljubljana, Ljubljana, Slovenia

³Institute of Oncology, Ljubljana, Slovenia

⁴Department of Abdominal Surgery, Division of Surgery, University Medical Centre, Ljubljana, Slovenia

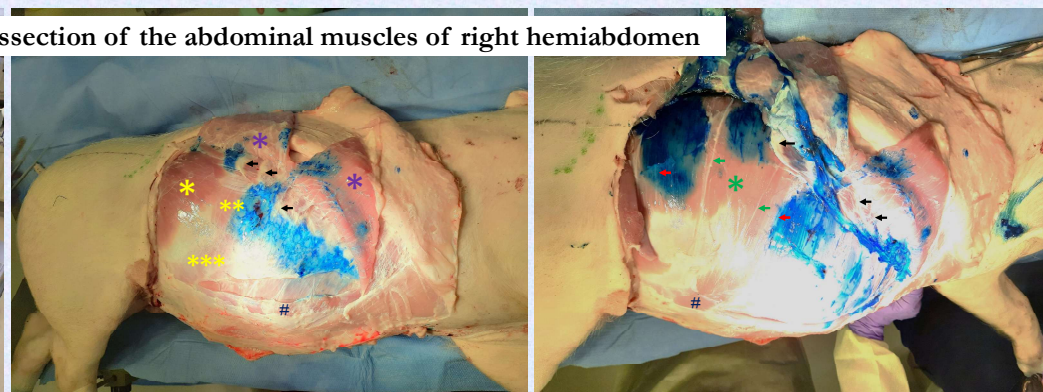
Transversus abdominis plane (TAP) block :

- used to desensitize the (caudal intercostal and lumbar) nerves of the abdominal wall
- an anaesthetic is administered interfascially between the *internal oblique muscle* and the *transversus abdominis muscle*.



X - 4 locations of TAP block administration at the left hemiabdomen

Anatomic dissection of the abdominal muscles of right hemiabdomen



The *external oblique muscle* (EOM, *) and *transversus abdominis muscle* (TAM, *) are mostly muscular. The muscular portion of the *internal oblique muscle* (IOM) is small and restricted to the paralumbar region (●). Its extensive aponeurosis is running cranioventrally and ventrally (■) and inherently connected to the aponeuroses of the EOM ventrally, the TAM cranially, or to the peritoneum ventrocaudally (■); *rectus abdominis muscle* (#), ribs (black arrow), an unstained nerve (→), a stained nerve (→).

TAP block performed on 10 pigs (*Sus scrofa domestica*):

(freshly euthanized) carcasses, and anaesthetized pigs

1. TAP block application with **methylene blue dye** (1 mg/kg in 5% glucose solution)
2. Anatomic dissection of the abdominal muscles of both hemiabdomens
3. The thoracic nerves were identified according to their position to the last rib and nerve staining assessed **5 minutes after removal** of the IOM from TAM

The study was approved by the National Veterinary Administration (U34401-2/2021/5) and conducted in accordance with Directive 2010/63/EU and ARRIVE 2.0 guidelines.

The aim of the study:

- an assessment of the anatomy of the abdominal wall in pigs
- enable a development of a **four-point TAP block technique**

Conclusions: The muscular part of the IOM is smaller and its aponeurosis more extensive than in other domestic animals, such as dogs. Methylene blue dilution successfully stained the tissue in freshly euthanized and anaesthetized animals and enabled evaluation of the TAP technique.

Microbiological air quality assessment as a refinement measure for the welfare of laboratory animals

Uroš Rajčević, Alenka Dovč, Katja Skulj and Gregor Jereb

INTRODUCTION

Refinement is the part of the 3Rs principle that could contribute most to improve the welfare of research animals housed in appropriate animal-assisted research facilities, since there is always an opportunity to improve the immediate environment of the research animals.

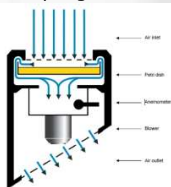
Animal research facilities house laboratory animals for breeding, experimentation, and resale. Air quality in such facilities is one of the most important parameters for a healthy environment. Microbiological air quality have therefore an important role.

AIM AND PURPOSE

In the present study, microbiological air quality was investigated in two animal research facilities. The main purpose was to evaluate the microbiological air quality and to exclude the possibility of spreading pathogens among laboratory mice via potentially contaminated air.

METHODS

Indoor bioaerosol measurements were made in the two experimental animal housing facilities. Airborne concentrations of bacteria and fungi were measured as CFU per 100 L of air. Samples of bio-aerosol were taken using a Merck MAS-100 NT bio-aerosol sampler. The microbiological air sampling is based on the impaction principle, sampler aspirates air through a perforated plate on to standard 90mm agar poured Petri dishes. The aspirated volume is a constant value of 100 liters per minute. 300 x 0.6mm sampling head (perforated lid) was used with declared impaction speed <20m/s.



RESULTS

The number of colonies in the air samples were shown as the measured number of colonies (CFU in the sample) and corrected as a probable number of colonies to a 1000 L (CFU/m³ after correction) using Feller conversion table for sampling head with 300 holes (MAS-100 NT™, 2008), prepared using Feller's equation (Feller, 1950).

Table 1: Microbiological air quality (sample represents 100 L of air)

Sample	Total CFU/m ³ (after Feller correction 1,2)	Location of sampling
AF1/8	260	Experimental room
AF1/16	330	Hallway/sanitary barrier
AF1/24	140	Breeding (transgenic mice)
AF2/32	40	Breeding (transgenic mice)
AF2/40	230	Hallway/sanitary barrier
AF2/48	50	Main room

Legend:

AF1 and AF2 - animal facility 1 and 2

The total number of bacteria and fungi in the air of the studied facilities did not exceed 300 CFU per 1 m³. The results indicate good microbiological air quality in both facilities studied, which could be due to excellent husbandry as well as adequate housing systems, although neither facility was housed in buildings primarily intended for laboratory animal husbandry.

CONCLUSION

Air quality monitoring could be a simple and, from the animals' point of view, non-invasive method to evaluate housing quality and one of the parameters indicating animal welfare.

Optimizing flow cytometry for genome size estimation in salamanders: a call for nondestructive methods in amphibian genomics

Vencelj Merc Bronja¹, Šimunović Katarina², Kladnik Aleš¹, Bizjak Mali Lilijana¹

¹Department of Biology, Biotechnical Faculty, University of Ljubljana, Ljubljana, Slovenia; ²Department of Microbiology, Biotechnical Faculty, University of Ljubljana, Ljubljana, Slovenia

Univerza v Ljubljani
Biotehniška fakulteta



We present a non-destructive method of estimating genome size in salamanders with flow cytometry, using propidium iodide-stained nuclei isolated from blood cells.



Image 1: The olm (*Proteus anguinus*)

References:

1. Deacon-Stephens, L. P., et al. Genome Size and Biological Size in a Diverse Clade of Salamanders. (2005)
2. Gavrilev, G. W. et al. Rapid Flow Cytometric Analysis of the Cell Cycle in Isolated Plant Tissues. (1993)
3. Sidiński, J. et al. Estimation of nuclear DNA content in plants using flow cytometry. (2007)

BACKGROUND

Salamanders (Urodela) possess some of the largest genomes among vertebrates, ranging from 9.3–120 gigabases (Gb). Genome size has been shown to strongly influence embryonic developmental time as well physical body and cell size and may serve as an important tool in research pertaining to evolution, phylogenetics and speciation of salamanders. Additionally, genome size is highly variable even among closely related taxons of salamanders – intraspecific genome size variance may thus help to elucidate taxonomic relationships among different subpopulations of species such as the endangered *Proteus anguinus*. Despite its great potential, research in the field of salamander genome size estimation has often been hampered by inconsistent, laborious and inappropriate methods. Sorely needed is a reliable protocol that provides consistent, comparable and accurate results. In our work, we present an efficient and simple method for estimating genome size in salamanders using flow cytometry.



Image 2: The Iberian ribbed newt (*Pleurodeles waltl*)



Image 3: The Axolotl (*Ambystoma mexicanum*)

METHODS

- The Iberian ribbed newt (*Pleurodeles waltl*), the Axolotl (*Ambystoma mexicanum*) and The olm (*Proteus anguinus*) were included in our study.
- Animals were anesthetized with 0.03-0.5% tricaine methanesulfonate (MS-222), buffered with sodium bicarbonate to a pH of 7.0-7.5.
- Blood was collected from the ventricle using a heparinized 26 G needle and a 1.0 mL syringe
- Nuclei of blood cells were extracted in Galbraith's lysis buffer for 30 minutes on ice and then stained with 100 µg/ml propidium iodide for an additional 30 minutes on ice and in the dark.
- Fluorescence was measured using a BD FACSMelody Cell Sorter.
- Genome size measurements were cross-checked using Feulgen densitometry
- Morphology of the stained nuclei was examined by fluorescence microscopy to verify the success of cell lysis.
- Various cell fixatives and parameters of sample preparation were assessed.

RESULTS, ASSAYED PARAMETERS

All specimens survived the blood taking; full recovery varied between individuals in the time frame of 10-40 minutes.

Comparison between DAPI and propidium iodide. Samples stained with 100 µg/mL of propidium iodide were compared with samples stained with a DAPI concentration of 4 µg/mL and 8 µg/mL. Compared to propidium iodide staining, DAPI staining resulted in poor separation of *P. waltl* and *A. mexicanum* peaks.

Comparison of different lysis treatments: Galbraith buffer was compared with a modified lysis buffer of 0.1% sodium citrate in 0.1% Triton X-100i. The modified lysis buffer did not prove to be a suitable substitute as it resulted in large cell nuclei aggregates.

Comparison of four cell fixation methods. Blood samples were fixed using four different treatments (70% EtOH, 3:1 methanol acetic acid, frozen at -20 °C in PBS with 1mM EDTA, 10% formalin). Samples were analyzed 7 and 14 days after fixation. This experiment is still in progress.

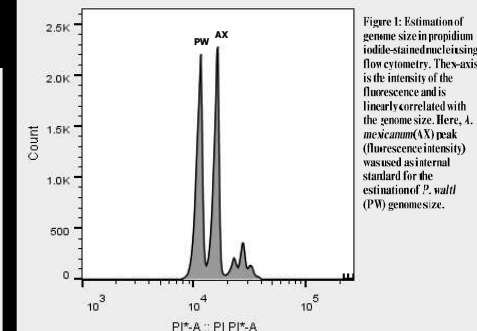


Figure 1: Estimation of genome size in propidium iodide-stained nuclei using flow cytometry. The y-axis is the intensity of the fluorescence and is linearly correlated with the genome size. Here, *A. mexicanum* (AX) peak (fluorescence intensity) was used as internal standard for the estimation of *P. waltl* (PW) genome size.

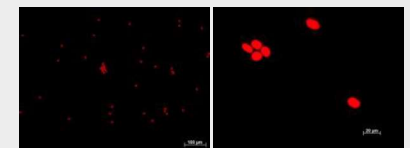


Image 4: *P. waltl* nuclei stained with propidium iodide (fluorescent microscopy)

An in vitro model reproducing the interactions between murine peritoneal macrophages and ovarian cancer cells

Simona Miceska^{a,b}, Vijayalaxmi Gupta^a, Bisiayo Fashemi^a, Tyler Woodard^a, Wendy Zhang^a, Dineo Khabele^a

^aWashington University School of Medicine, St. Louis, MO, USA, ^bInstitute of Oncology Ljubljana, Slovenia



INTRODUCTION

Tumor-associated macrophages (TAMs) are a major component of ascites microenvironment in ovarian cancer (OC), affecting spheroid formation and tumor growth. However, established techniques for studying the impact of TAMs on biological behavior of OC cells in vitro are limited. Our objective was to create a 3D in vitro model that can reproduce the in vivo interactions of TAMs and OC cells. Our aims were to test and compare two different in vitro 3D co-culturing models of OC and macrophages, and to induce in vitro polarization of the macrophages from M1 to M2-like type and observe its effect in co-culture.

METHODS

To mimic ascites microenvironment, murine ID8 p53 null OC cells and peritoneal macrophages PMJ2-R were co-cultured at ratio 10:1. Ultra-low attachment surface coated- and 0.5% Matrigel-coated 96-well plate spheroid formation methods were compared. Separately cultured PMJ2-R and ID8 p53 null were used as a control. Different staining and visualization techniques (H&E, immunocytochemistry, immunofluorescence, live cell tracking) were used to quantify the spheroids with both methods. PMJ2R polarization from M1-like to M2-like phenotype was achieved by 48h pre-treatment with IL-4. TAM The expression of TAMs specific markers (CCL3, CD206, F4/80) was studied using RT qPCR. PMJ2R cytokine expression level was analyzed by ELISA cytokine array.

RESULTS

Matrigel co-culturing method induced formation of multiple ID8 p53 null and PMJ2R single spheroids, with variable and smaller size compared to the heterospheroid, stimulated by low-attachment method (Figure 1).

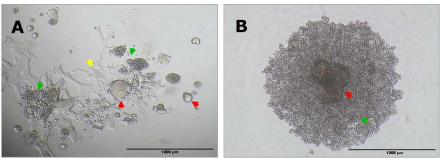


Figure 1: Morphology of A) matrigel spheroids at one week and B) low-attachment spheroids at 72 hours. Red arrows are indicating ID8 p53 null spheroids, and green are indicating PMJ2R macrophages. 50x magnification.

RESULTS

Low-attachment co-culturing method was better for quantification and analysis of the development and growth of ID8 p53 null OC and PMJ2R macrophages within the heterospheroid. Although different visualization techniques were applied (Figure 2, Figure 3) real time microscopy was the most representable and easy way for quantification (Figure 3).

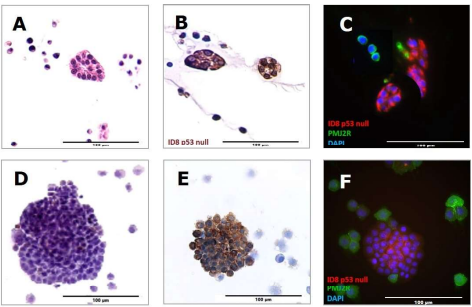


Figure 2: Techniques used for visualizing co-cultured spheroids. FFPE matrigel sections stained with A) H&E, B) epithelial marker CK8 (brown, immunohistochemistry), C) epithelial marker CK8 (red) and macrophage marker F4/80 (green, immunofluorescence), ice-cold fixed low-attachment spheroid cytopins, stained with D)H&E, E) epithelial marker CK8 (brown, immunohistochemistry), F) epithelial marker CK8 (red) and macrophage marker F4/80 (green, immunofluorescence). 200x magnification.

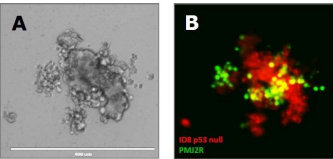


Figure 3: Real-time cell tracking of the low-attachment heterospheroid. A) light microscopy. B) Cell tracking of the ID8 p53 null cells (red cell tracker) and PMJ2R macrophages (green cell tracker). 100x magnification.

ID8 p53 null OC had better growth in co-culture with M1-like and M2-like PMJ2R macrophages in low-attachment growth conditions compared to the control (ID8 p53 null monoculture). However, M2-like PMJ2R macrophages induced better growth of the heterospheroid compared to M1-like PMJ2R (Figure 5).

RESULTS

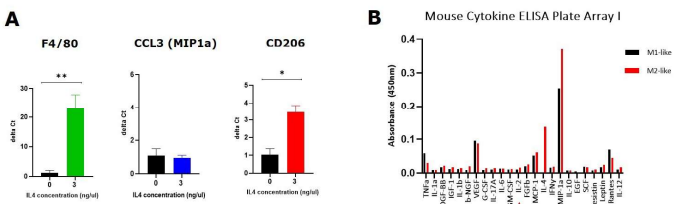


Figure 5: A) Treatment with IL-4 significantly increased the expression of pan-macrophage marker F4/80 and mannose receptor CD206 (M2 marker) but did not affect the expression of chemokine ligand CCL3 (M1 marker) after 72h. B) Cytokine profile of M1-like and M2-like PMJ2R macrophages after 48h IL-4 treatment.

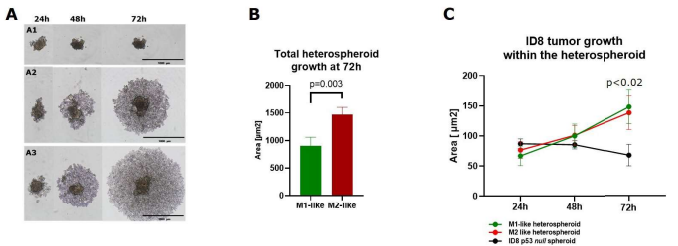


Figure 6: Comparison of M1-like and M2 like heterospheroid growth. A) The growth of A1) ID8 p53 null spheroid alone, A2) M1-like heterospheroid, A3) M2-like heterospheroid. 50x magnification. B) The area of the ID8 p53 tumor growth within the heterospheroid growth from 24-72h. C) The area of the total heterospheroid growth at 72h.

CONCLUSION

The low-attachment co-culturing 3D method allowed easier quantification of tumor cell growth along with the growth of the heterospheroid compared to matrigel method and may be beneficial for studying the interactions of TAMs and ovarian cancer cells in vitro.





Katerina Jazbec, **Simona Miceska**, Mojca Jež, Urban Švajger, Boštjan Smrekar, Uroš Rajčević, Mojca Justin, Janja Završnik, Tadej Malovrh, Mitja Gombač, Živa Ramšak, Primož Rožman

Blood Transfusion Centre of Ljubljana, Slovenia

The stem cell theory of aging postulates that stem cells become inefficient at maintaining the original functions of the tissues. We, therefore, hypothesized that transplanting young bone marrow (BM) to old recipients would lead to rejuvenating effects on immunity, followed by improved general health, decreased frailty, and possibly life span extension.

The stem cell theory of aging postulates that stem cells become inefficient at maintaining the original functions of the tissues. We, therefore, hypothesized that transplanting young bone marrow (BM) to old recipients would lead to rejuvenating effects on immunity, followed by improved general health, decreased frailty, and possibly life span extension.

The old mice developed $18.7 \pm 9.6\%$ donor chimerism in the BM and showed favorable counts of neutrophils in the spleen and BM, central memory Th cells, effector/effector memory Th and Tc cells in the spleen, and B1a and B1b cells in the peritoneal cavity, as well as enhanced borderline lymphocyte proliferation capacity. There were no differences between frailty parameters, pathomorphological results, and life spans among transplanted and control group of mice.

The old mice developed $18.7 \pm 9.6\%$ donor chimerism in the BM and showed favorable counts of neutrophils in the spleen and BM, central memory Th cells, effector/effector memory Th and Tc cells in the spleen, and B1a and B1b cells in the peritoneal cavity, as well as enhanced borderline lymphocyte proliferation capacity. There were no differences between frailty parameters, pathomorphological results, and life spans among transplanted and control group of mice.

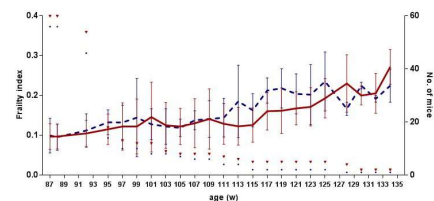


Figure 3. Frailty index (FI) results are shown in the combined plot. The x-axis shows the age of mice in weeks, the y-axis (left) shows FI (\pm SD) values, and (right) the number of analyzed mice. Legend: Solid line—BMT-transplanted aged group, dashed line—SHAM-aged control group, \circ —number of evaluated BMT mice, number of evaluated SHAM mice.

Tables 1-3. Immunophenotyping by flow cytometry (cell sources: spleen (Table 1), bone marrow (Table 2) and peritoneal cavity (Table 3))

[illegible]

A murine model of non-myceloablative heterochronic BM transplantation was developed, in which old female BALB/c mice at 14, 16, and 18(19) months of age received $125.1 \pm 15.6 \times 10^6$ nucleated BM cells from young male donors aged 7-13 weeks. At 21 months, donor chimerism was determined, and the immune system's innate and adaptive arms were analyzed. Mice were then observed for general health and frailty until spontaneous death, when their lifespan, post-mortem examinations, and histo-pathological changes were recorded.

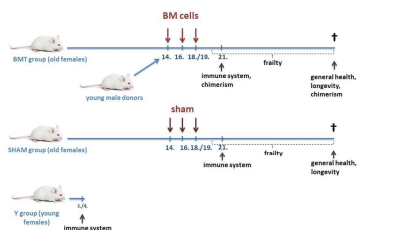


Figure 1: Experimental scheme of the study. The numbers indicate mice age in months, 'BM cells' indicate the time of BM transplantations (BMT), and sham indicate DPBS injections. Legend: BMT group - received BMT, SHAM group - control group, and Y group - control group of young female mice. Abbreviations: BM, bone marrow; BMT, BM transplantation.

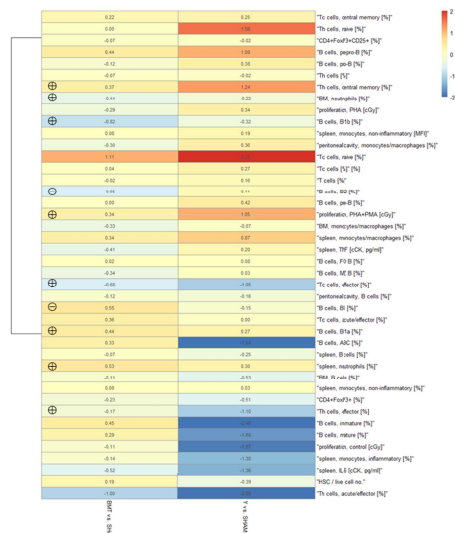


Figure 2. Heatmap of the analyzed parameters. The types of analysis are shown along the right axis, group comparison along the bottom axis. Red results indicate that the result is higher than in the SHAM group, and blue results indicate that the result is lower than in the SHAM group. Numbers in the boxes indicate the factor: 1 means the result is two times higher, and -1 indicates that the result is two times lower. Legend: BMT-transplanted aged mice, SHAM-aged control mice, Y-young control mice, @ rejuvenation effect, @ adverse effect.

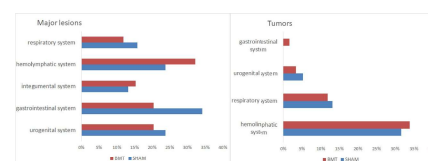


Figure 4. Results of pathomorphological analyses of the aged mice that received heterochronic BM transplantation (BMT, $n = 59$) and of the aged control mice (SHAM, $n = 38$); (left) the percentage of major lesions in different organ systems; (right) the percentage of tumors in different organ systems.

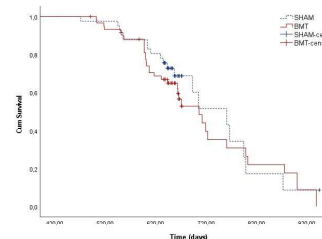


Figure 5. Kaplan-Meier survival curves. The equality test showed no significant differences between the transplanted group (BMT) and the control group (SHAM). BMT-censored and SHAM-censored are the mice that died during the transplantation process or were deliberately euthanized for the immune system analyses.

Our heterochronic non-myeloablative transplantation model showed certain improvements in the innate and adaptive immune system. However, additional optimization is needed to achieve better rejuvenation effects.



Scan me!

Kate Šešelja 1, Iva Bazina 1, Milka Vrecl 2, Jessica Welss 3, Martin Schicht 3, Friedrich Paulsen 3, Mirela Baus Lončar 1 and Tatjana Pirman 4

1 Department of Molecular Medicine, Division of molecular medicine, Ruđer Bošković Institute, Bjenička 54, 10 000 Zagreb, Croatia; 2 Institute of Preclinical Sciences, Veterinary Faculty, University of Ljubljana, Gerbičeva 60, 1000 Ljubljana; Slovenia; 3 Institute of Functional and Clinical Anatomy, Faculty of Medicine, Friedrich-Alexander-University Erlangen-Nürnberg, 91054 Erlangen, Germany; 4 Department of Animal Science, Biotechnical Faculty, University of Ljubljana, Groblje 3, 1230 Domžale, Slovenia;

INTRODUCTION

Trefoil factor family protein 3 (*Tff3*) is a small peptide found mainly in the gastrointestinal mucosa and is involved in epithelial restitution, influencing apoptosis, and immunologically relevant signaling pathways. Its **wide distribution** in blood, liver, bile, pancreas, brain, exocrine and endocrine signaling pathways, as well as its ability to bind to different partners, contribute to the complex mode of action of the *Tff3* protein in various tissues and the gut-liver-brain axis.

We have developed a new *Tff3*-deficient mouse strain (*Tff3*^{-/-}/*C57BL6NCrl*) from an existing mixed strain (sv129/*C57BL/6J*) (1). Mice with *C57BL/6J* background have an additional genetic variation in the nicotinamide nucleotide transhydrogenase (*Nnt*) gene, which encodes the mitochondrial redox-induced proton pump that links NADPH synthesis to the mitochondrial metabolic pathway. Deletion of *Nnt* modulates metabolism [2] and immune response [3] and conceals the physiological function of the candidate protein under study.

Here, we describe the effects of *Tff3* deficiency on intestinal tissue in the case of a **prolonged high-fat diet** (HFD), a widely accepted model of metabolic stress affecting the gut-liver-brain axis.

METHOD

We have examined the effects of prolonged HFD exposure (30 weeks) on male ♂ and female ♀ wild-type (Wt; *C57BL6N Crl*) and *Tff3*-deficient mice (*Tff3*^{-/-}/*C57BL6NCrl*).

Specifically, we examined the **effects of *Tff3* deficiency on intestinal morphology and ultrastructure** and short-chain fatty acid content as indicators of the microbiome. **Metabolic pathways related to *Tff3* function** (oxidative and endoplasmic reticulum stress (ER) and inflammation) were monitored by Sybergreen-based QPCR expression analysis. Data were analyzed using REST® software (ΔΔCt method) and changes were presented as log2 (fold change) using the stable reference genes (*ACTB* and *B2M*).

RESULTS

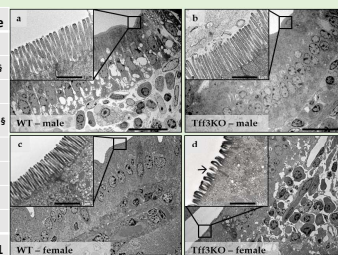
A					B			
Intestinal histology	Wt male	<i>Tff3</i> ^{-/-} male	Wt female	<i>Tff3</i> ^{-/-} female	a		b	
Duodenum								
Villi height (μm)	420.6 ± 83.2 *	501.6 ± 31.2 *	531.7 ± 60.5	416.8 ± 33.6 §				
Villi average diameter (μm)	255 ± 31	278 ± 29	292 ± 26	249 ± 19 §				
Villi area (μm²)	57321 ± 19416	62933 ± 1270	68475 ± 1224	49855 ± 7558 §				
Ratio villi height : diameter	1.64 : 1	1.81 : 1	1.82 : 1	1.68 : 1				
Crypt depth	70.5 ± 5.0	77.1 ± 1.5 ‡	73.3 ± 6.0	71.7 ± 7.5				
Ratio villi : crypt	5.9 : 1 *	6.5 : 1	7.3 : 1	5.9 : 1 §				
Caecum								
Crypt depth	166.2 ± 20.2 *	140.8 ± 12.0 **	213.9 ± 26.1	9. ± 17.1				

Figure 1. A. Histological measurements of duodenum and caecum (average ± standard deviation) of HFD exposed mice. Results are presented as average ± standard deviation. Statistical significance was considered at $p \leq 0.05$: * - Wt ♂ vs Wt ♀ (sex-related diff.) ‡ - *Tff3*^{-/-} ♂ vs *Tff3*^{-/-} ♀ (sex-related diff.) § - Wt ♂ vs *Tff3*^{-/-} ♀ (gene-related diff.) ¶ - *Tff3*^{-/-} ♂ vs *Tff3*^{-/-} ♀ (gene-related diff.). **B.** Duodenal ultrastructure of Wt and *Tff3*^{-/-} mice exposed to HFD. (a) Wt male ♂; (b) *Tff3*^{-/-} male ♂; (c) Wt female ♀; (d) *Tff3*^{-/-} female ♀. Length of the microvilli in the duodenum of *Tff3*^{-/-} mice is reduced (→); scale bars 20 μm and 1 μm (inserts).

CONCLUSION

Prolonged HFD induced **differential effects on gut structure in *Tff3*-deficient male and female mice**. For the first time, we found a sex-specific difference in duodenal morphology after prolonged HFD.

***Tff3*-deficient ♂ compared with Wt ♂, had reduced microvilli height. These changes could not be attributed to alterations in the monitored genes for ER and oxidative stress, and inflammation.**

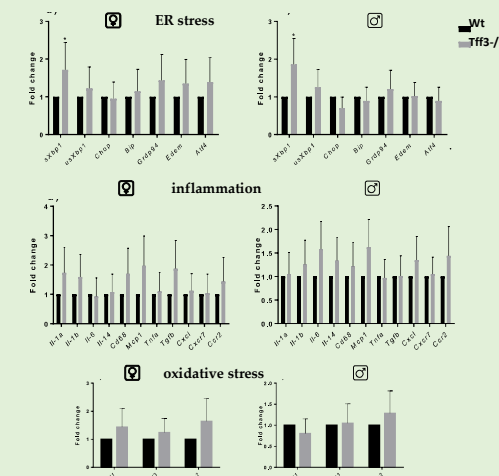
Tff3-deficient ♀ exhibited reduced depth of the cecal crypt compared with Wt ♀, which was not the case in ♂.

Microbiome-related short-chain fatty acid content was not affected by *Tff3* deficiency in both sex mice exposed to HFD.

The sex differences due to *Tff3* deficiency make it necessary to consider both sexes in future studies on the role of Tffs in gut function.

Short chain fatty acids	Wt ♂	<i>Tff3</i> ^{-/-} ♂	Wt ♀	<i>Tff3</i> ^{-/-} ♀
Acetic acid	1.80 ± 0.85	1.66 ± 0.46	1.99 ± 0.47	1.81 ± 0.41
Propionic acid	0.34 ± 0.12	0.38 ± 0.11	0.47 ± 0.10	0.42 ± 0.09
i-Butyric acid	0.04 ± 0.03	0.04 ± 0.02	0.04 ± 0.02	0.05 ± 0.01
n-butyric acid	0.24 ± 0.15	0.29 ± 0.11	0.28 ± 0.09	0.30 ± 0.12
i-valerianic acid	0.05 ± 0.03	0.06 ± 0.03	0.06 ± 0.02	0.06 ± 0.01
n-valerianic acid	0.05 ± 0.03	0.05 ± 0.02	0.06 ± 0.02	0.06 ± 0.02
Sum	2.52 ± 1.13	2.49 ± 0.68	2.90 ± 0.57	2.70 ± 0.61
Ratio AA : PA : BA	5.33 : 1 : 0.80	4.77 : 1 : 0.90	4.31 : 1 : 0.68	4.33 : 1 : 0.82

Figure 2. Short chain fatty acid concentration (g/kg sample) in caecum. Results are presented as average ± standard deviation. AA – acetic acid; PA – propionic acid; BA – butyric acid.



Effect of Trefoil factor 3 deficiency in hippocampus of mice on short-term high fat diet

Šešelja Kate 1, Bazina Iva 1, Baus Lončar Mirela 1,

1 Division of Molecular Medicine, Laboratory for Neurodegenerative Disease Research, Ruder Bošković Institute, Bijenicka 54, 10000 Zagreb, Croatia

Introduction

Trefoil factor 3 (Tff3) is a small secretory peptide found primarily in the gastrointestinal tract (GI), where it plays a role in epithelial protection through its involvement in various physiological processes, including cell migration and immune response. However, Tff3 is also expressed in neurons in many adult and developing brain regions, as well as in astrocytes and microglia in primary cultures(1). In recent years it has been shown that **Tff3 may play an important role in neurodegenerative diseases, including Alzheimer's disease (AD)**. Tff3 was significantly reduced in cerebrospinal fluid of AD patients, and low levels correlated with whole brain atrophy, hippocampal atrophy, and ventricular expansion (2). Intraperitoneal administration of Tff3 improved learning and memory performance in mouse models (3).

Our goal was to examine possible differences in phenotype caused by Tff3 deficiency in the early phase (activation of neurodegenerative processes) **with a focus on hippocampus integrity(adult neurogenesis/neuroinflammation) after short-term high-fat diet treatment.**

Study design

Short-term HFD has been shown to significantly affect **neurogenesis and neuroinflammation; two relevant hallmarks of AD**. Newly developed congenic *Tff3*^{-/-} (C57BL/6N) ♂ and ♀ mice and WT controls were exposed to 9 weeks of HFD treatment. We analyzed relevant markers of neurogenesis and neuroinflammation (WB, IHC method) in the hippocampus of the mouse models. We focused on neurogenesis and neuroinflammation because of the known role of Tff3 in cell migration and inflammatory response in the GI tract.

REFERENCES

- (1) Gert, H.; Henrik, B.; Trübner, K.; Steiner, J.; Bogerts, B. Differential regional and cellular distribution of TFF3 peptide in the human brain. **2015**
- (2) Paterson, R.W.; Bartlett, J.W.; Blennow, K.; Fox, N.C.; Shaw, L.M.; Trojanowski, J.Q.; Zetterberg, H.; Schott, J.M. Cerebrospinal fluid markers including trefoil factor 3 are associated with neurodegeneration in amyloid-positive individuals. *Transl. Psychiatry* **2014**
- (3) Shi, H.S.; Yin, X.; Song, L.; Guo, Q.J.; Luo, X.H. Neuropeptide Trefoil factor 3 improves learning and retention of novel object recognition memory in mice. *Behav. Brain Res.* **2012**

Results

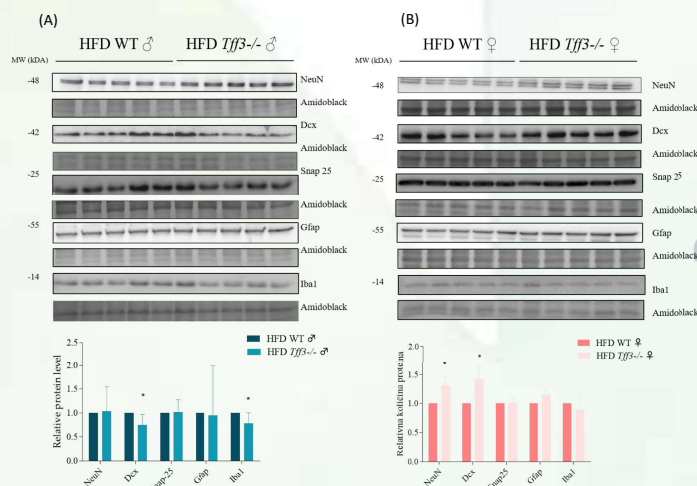


Figure 1. Protein level of NeuN, Dcx, Snap-25, Iba1 and Gfap was determined by Western blot in the hippocampus of WT (C57BL/6N) and *Tff3*^{-/-} ♂ (A) and ♀ (B) mice fed with HFD for 9 weeks. Protein level is presented relative to WT mice as mean ± SEM of specific protein band density normalized with amido black. The differences between groups were compared by the Student t-test and presented as *p < 0.05.

Summary and conclusion

After 9 weeks of HFD, the **marker of immature neurons (Dcx)** and marker of **microglia (Iba1)** is significantly reduced in the hippocampus of *Tff3*^{-/-} male mice compared with WT male, but surprisingly the opposite effect is detected in the hippocampus of *Tff3*^{-/-} female mice which had a significant increase in Dcx and marker of **mature neurons (NeuN)**. We found for the first time that **Tff3 may play a role in adult neurogenesis under relevant metabolic conditions**, which opens a new field of research with the aim of elucidating the precise role of Tff3 in these processes and potentially discovering new therapeutic targets. Moreover, the observed phenotypes differ significantly by sex, highlighting **the need to include both sexes in future research on the role of Tff3.**

After 9 weeks of HFD →
Tff3^{-/-} ♂ → decreased rate of hippocampal adult neurogenesis

Tff3^{-/-} ♀ → increased rate of hippocampal adult neurogenesis

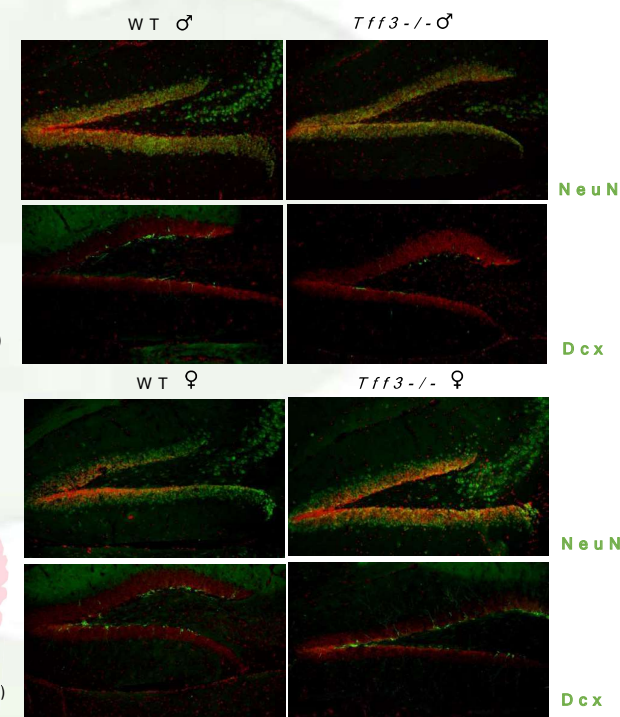


Figure 2. Visualization of NeuN and Dcx in hippocampus of WT (C57BL/6N) and *Tff3*^{-/-} ♂ (A) and ♀ (B) mice fed with HFD for 9 week. Each image is merged with DAPI(nuclei stain- red) and NeuN and Dcx signals are marked with green

ACKNOWLEDGMENTS

This work was supported by Croatian Science Foundation grant IP-06-2016-2717 and "Young researchers career development project – training of doctoral students" of the Croatian Science Foundation funded by the European Union from the European Social Fund (I.Bazina)

A mouse model of HPV-positive head and neck cancer: development and characterisation

Ziva MODIC^{1,2}, Maja CEMAZAR^{1,3}, Bostjan MARKELC¹, Andrej CÖR^{4,5}, Gregor SERSA^{1,6}, Simona KRANJC BREZAR^{1,2}, Teja VALANT¹, Tanja JESENKO^{1,2}

¹ Department of Experimental Oncology, Institute of Oncology Ljubljana, Ljubljana, Slovenia; ² University of Ljubljana, Faculty of Medicine, Ljubljana, Slovenia; ³ University of Primorska, Faculty of Health Sciences, Izola, Slovenia; ⁴ University of Ljubljana, Faculty of Health Sciences, Ljubljana, Slovenia; ⁵ Department of Research, Valodtra Orthopedic Hospital, Ankaran, Slovenia; ⁶ University of Primorska, Faculty of Education, Koper, Slovenia

This work received funding from Slovenian Research Agency (ARRS) under research programme P3-0003, bilateral research project funding BT-AT/23-24-027, and ARRS postgraduate programme.

zmodic@onko-i.si

CONCLUSIONS

The established MOC1-HPV mouse model of HPV-positive oral squamous cell carcinoma (OSCC) can be used to study tumour microenvironment and immune responses of HPV-positive OSCC. *In vitro* we observed differences in cell migration. *In vivo*, MOC1-HPV K1 mouse model showed increased sensitivity to irradiation and differed from the HPV-negative counterpart in the extent of hypoxia and proliferating cells. The observed differences are in line with the results of transcriptome analysis.

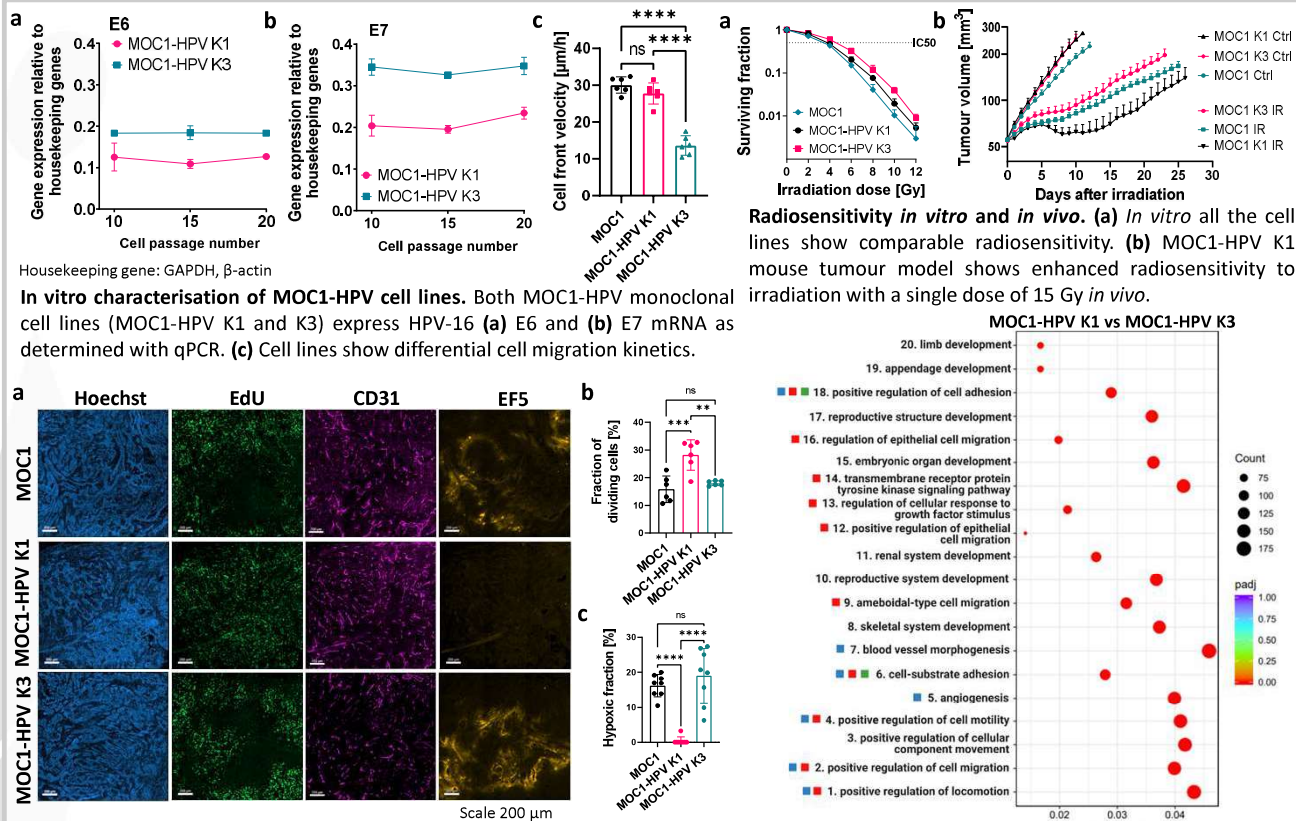
BACKGROUND

It has been shown that infection with high-risk types of HPV correlates with the development and differential radiosensitivity of some OSCC. However, due to the species specificity of HPV, HPV-positive mouse models of OSCC for *in vivo* evaluation of therapies based on adaptive immune responses are still scarce.

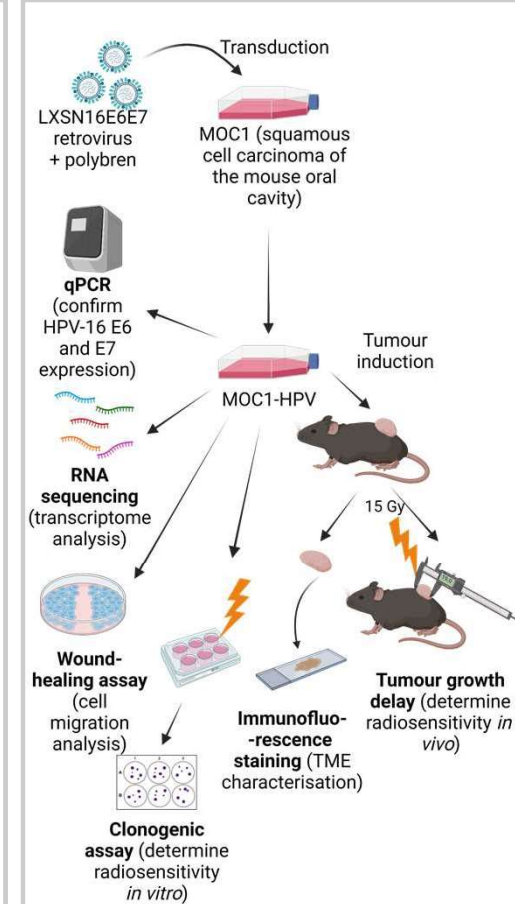
OBJECTIVES

Our study aimed to establish and characterise a mouse model of HPV-positive OSCC.

RESULTS



METHODS



The feasibility of gene electrotransfer for vaccination against COVID-19

Simona Kranjc Brezar¹, Urška Kamenšek^{1,2}, Tanja Jesenko¹, Maja Čemažar^{1,3}, Špela Kos¹, Boštjan Markelc^{1,4}, Katarina Žnidar¹, Živa Modic¹, Tilen Komel¹, Eva Reberšek², Helena Jakopič², Tim Gorše², Gregor Serša^{1,4}

ONKOLOŠKI INŠTITUT
INSTITUTE OF ONCOLOGY
LJUBLJANA

¹Institute of Oncology Ljubljana; ²Biotechnical Faculty, University of Ljubljana; ³Faculty of Health Sciences, University of Primorska; ⁴Faculty of Health Sciences, University of Ljubljana
skranjc@onko-lj.si

Universita v Ljubljani

UIO

ARRS

REPUBLIC OF SLOVENIA
MINISTRY OF EDUCATION,
SCIENCE AND SPORT

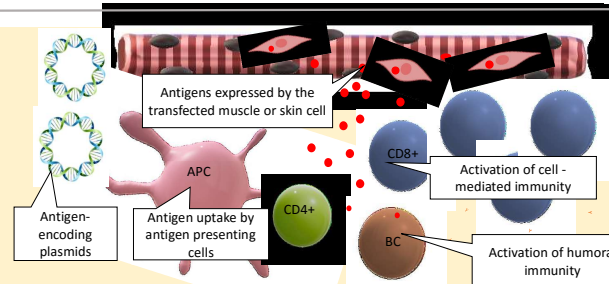
European Union
European Regional
Development Fund
Investing in your future

SmartGene.si

SmartGene.si

Introduction and aim

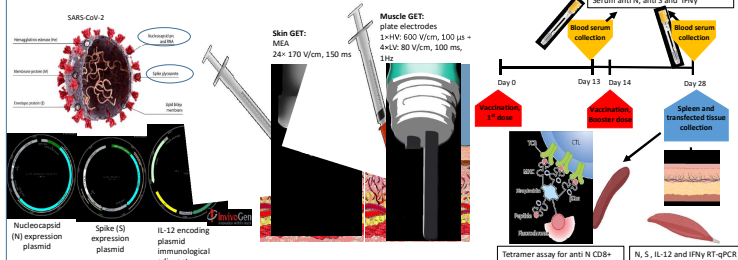
DNA vaccination is one of the emerging approaches for vaccination against COVID-19 and other diseases. The aim of this study was to investigate the feasibility of Gene Electro Transfer (GET) in the context of vaccination against COVID-19.



Conclusions

Vaccination using GET was well tolerated and led to a significant induction of humoral and cell-mediated immunity, confirming the feasibility of GET platform for DNA vaccination against infectious disease like COVID-19.

Materials and methods



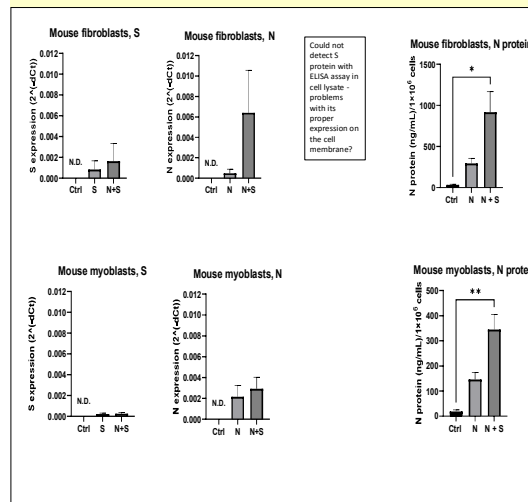
Two plasmids encoding SARS-CoV-2 spike (S) or nucleocapsid (N) protein were used as the source of antigens. Additionally, an interleukin 12 (IL-12)-encoding plasmid was used as an immunological adjuvant in the *in vivo* experiments. The expression of N and S proteins after *in vitro* GET in mouse myoblast cell line C2C12 and fibroblast cell line L929 was assessed by RT-qPCR and ELISA assays. *In vivo* vaccination was performed via GET of 45 μg of plasmid DNA in the skin or muscle tissue of C57BL/6J mice on days 0 and 14 (boost). Two weeks after the boost, blood, spleens and transfected skin or muscle tissue were collected. Expression of S, N, IL-12 and interferon γ (IFN-γ) in the transfected tissue was determined by RT-qPCR, and IFN-γ in serum by ELISA. Induction of antigen-specific IgG antibodies was determined by ELISAs, and induction of antigen-specific cytotoxic T cells by tetramer assay on isolated splenocytes.

Results

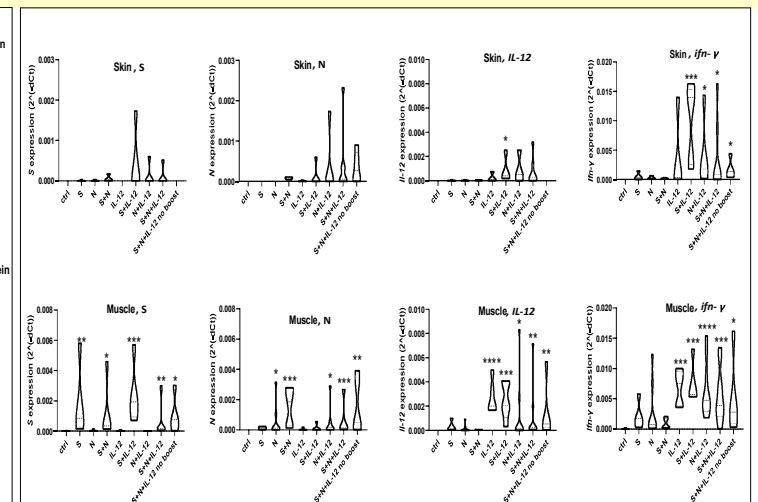
We confirmed that both *in vitro* and *in vivo* GET leads to expression from transfected plasmids. Production of N was further confirmed on protein level, while S was not detectable using available ELISA kits, indicating problems with its proper presentation on the cell membrane. Indeed, vaccination with S did not lead to the induction of S-specific antibodies. Vaccination with N, however, led to a significant induction of N-specific antibodies. Intramuscular vaccination proved superior to skin vaccination, therefore test for cell-mediated immunity were performed only after intramuscular vaccination using only the plasmid for N. Final results confirmed that intramuscular vaccination with GET of N-encoding plasmid led to formation of antigen specific antibodies against the presented antigen as well as induction of N-specific cytotoxic T cells, which was significantly higher when IL-12 was used as immunological adjuvant.

Results

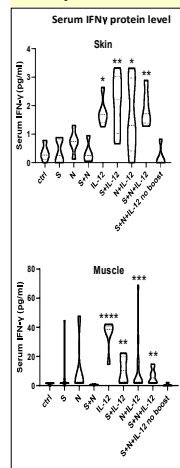
Expression *in vitro*



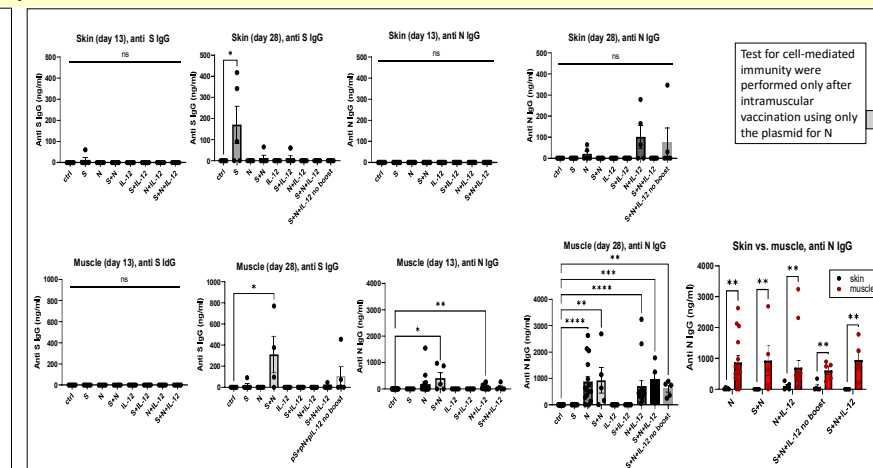
Expression *in vivo*



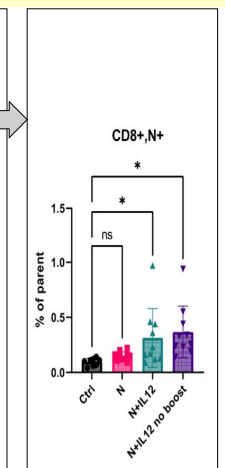
Non-specific immunity



Humoral immunity



Cell-mediated immunity





biomedicines

an Open Access Journal by MDPI

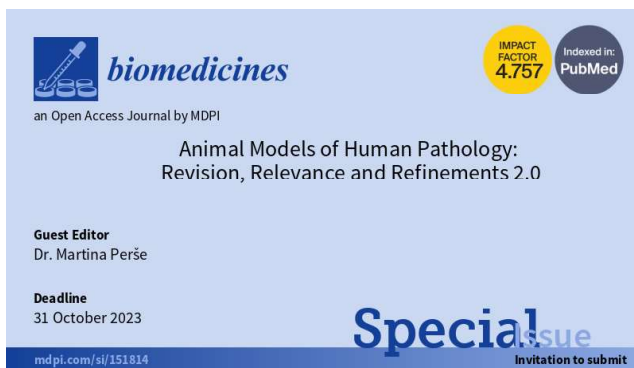


Special Issue Title: Animal Models of Human Pathology: Revision, Relevance and Refinements 2.0

Guest Editors: Dr. Martina Perše

We aim to collect submissions of basic research using animal models to understand diseases and underlying mechanisms or to investigate new treatment strategies in various human diseases. New approaches towards the use of animal models or refinements of particular animal models of human pathology as well as methodological and welfare are also welcome.

Submission Deadline: 31 October 2023



Biomedicines Editorial Office
St. Alban-Anlage 66
4052, Basel, Switzerland

✉ biomedicines@mdpi.com
▶ www.mdpi.com/journal/biomedicines
🐦 @Biomed_MDPI



More than 10 million animals per year are bred-but-not-used (surplus) for research in the EU^{1,2}

1. https://ec.europa.eu/environment/chemicals/lab_animals/pdf/SWD_part_C.PDF
2. <https://eur-lex.europa.eu/legal-content/EN/TXT/PDF/?uri=CELEX:52020SC0015>

Every facility is working hard on reducing surplus animals.



In case there is surplus, the **Biotech-Xchange.com platform** can help with reducing this number



Biotech-Xchange.com is a solid platform **intended for the global laboratory animal science community**



The more LAS colleagues use the platform the more effective the service becomes in **helping to reduce the number of surplus animals**



Use the platform also to **share alternatives to animal testing** and to find **innovative 3R solutions**



This platform is **only accessible by invite**: once you have joined you can simply invite your other colleagues with one click



Furthermore, the platform is the **perfect place to share information** on other products, services, courses and vacancies that are relevant for the LAS community

<https://qrco.de/bdsA8u>
<https://www.biotech-xchange.com>



Scan Your Invite



BIOTECH-XCHANGE.COM



15th June 2023

Congress on LAS in Ljubljana



WELCOME



**Improving nonclinical research practices:
the way forward**

LAS in Slovenia and SLAS



27th October 2001 – Seminar with international participation – idea on SLAS establishment - 2003

Legislation in Slovenia (based on Directive 86/609/EEC)

1986 – Instructions on conditions for granting authorizations for experiments on animals for scientific and research purposes

1999 – Animal Protection Act

2000 – Rules on the Ethical Commission for the experiments on animals

2004 – Rules on conditions for experiments on animals

2007 – Rules on methods of killing of experimental animals



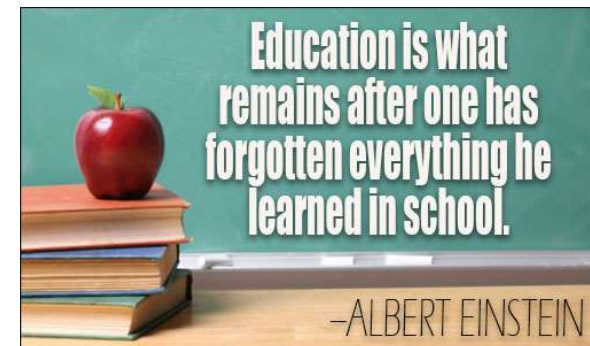
2005 - National Ethical Committee for project evaluation

2007 – Courses on LAS in Slovenia

2010 - Directive 2010/63/EU

October 2010: SLAS restored to life

April 2012 - SLAS election and activation



SLAS past activities



January 2013: The 1st Congress of SLAS



November 2013: Novel legislation and its interpretation in practice (workshop)

June 2014: The 2nd Congress of SLAS



March 2015: Humane end points in animal experimentation (workshop)

March 2016: **round table: Animal experimentation: need or unnecessary luxury.** The event was organized for the public; it was run by a journalist from national TV (the journalist responsible for documentary series titled Science on the street) and was recorded.

June, 2016: Work with genetically altered animals used for scientific purposes (workshop)

October, 2016: Anatomy and pathohistology of laboratory mouse (workshop)

January, 2017: Microbiological and Nutritional standards for laboratory rodents (workshop) SLAS and CroLASA (51 participants);

June, 2017: The 3rd Congress of SLAS and 1st joint SLAS-CroLASA (82 participants)



The FELASA Severity Assessment/Classification Workshop (47 participants)

November, 2017: Surgical procedures and peri-operative care of mice and rats (workshop, 42 participants)

March, 2018: Aging processes in Laboratory Rodents (workshop, 30 participants)

June, 2018: The 4th Congress of SLAS (91 participants)



October, 2018, Zagreb: The 3rd Congress of CroLASA and 2nd joint CroLASA-SLAS meeting (91 participants)

2019: Call for a 3R award (the award was 200 EUR for organization)

SLAS past activities



March, 2019: Monitoring and classification of actual severity (workshop, 29 participants);

June, 2019: New methods of handling for laboratory mice (workshop, 40 participants);

July, 2019: Monitoring and classification of actual severity (organized only for members of Ethical Committee for experiments on animals, 5 participants).

November, 2019: Factors affecting reproducibility of biomedical research on animals (workshop, 50 participants).

January, 2020: **Animal experimentation:** documentary series **run on national TV**. [Poskusi na živalih \(rtvslo.si\)](https://www.rtv.slo.si/poskusi-na-zivalih)

November, 2020: webinar: **Impact of genetic factors on animal research results** (65 participants);

March, 2021: webinar: **Refinement implementation in care and procedures: examples in laboratory rodents** (92 participants)

April, 2021: webinar: **National legislation: competence conditions for personnel working with animals** (132 participants);

June, 2021: webinar: **Applying aseptic conditions in rodent surgeries – yes we can!** (67 participants);

November, 2021: webinar: **The path to good reporting of animal experiments** (81 participants);

December, 2021: webinar: **Anesthesia and analgesia of pigs and sheep in research** (49 participants);

2021: Call for 3 financial awards for reporting quality of animal experiments

(the award was a registration fee for FELASA Congress 2022 – 600 EUR)

2022: Call for 3 financial awards for reporting quality of animal experiments

(the award was 200 EUR for organization)

SLAS



2016 - a member of FELASA



2022 - a member of ICLAS



2022 - a member of EARA





SLAS-CroLASA collaborations



January, 2017: Microbiological and Nutritional standards for laboratory rodents (workshop) SLAS and CroLASA (51 participants)

June, 2017: The 3rd Congress of SLAS and 1st joint SLAS-CroLASA (82 participants);
The FELASA Severity Assessment/Classification Workshop (47 participants)



October, 2018, Zagreb: The 3rd Congress of CroLASA and 2nd joint CroLASA-SLAS meeting (91 participants).



2022 LAS WEBINARS

PROGRAMME

"Improving nonclinical research practices: way forward"

1st LAS WEBINAR

16th February 2022

ČAS / TIME	TEMA / TOPIC	PREDAVATELJ/SPEAKER
14 ⁰⁰ - 14 ³⁰	Introduction	CroLASA & SLAS



CroLASA past activities

1980 - Croatian LAS started, some 20 LAS professionals gathered as a small section of the Croatian Physiological Society

1990 - Croatian Association for LAS (CroLAS) was constituted as an stand alone association

1999 - became ICLAS member



2007 - the FELASA member

renamed to CroLASA and gained momentum and larger membership





LAS in Croatia and CroLASA

2013 - Croatia joined the EU,
the **Directive 2010/63/EU** transposed into the national legislation

- constitution of the **National Ethics Committee** and registration of a number of **national LAS course** providers endorsed by the National Competent Authority, Ministry of Agriculture

2017 - CroLASA joined the established course providers in continuous professional development activities by organizing a series of congresses, compliant with the 2010/63/EU requirements, some of them in collaboration with the SLAS

- this trend was discontinued due to pandemic resulting in transfer of activities on-line, aided by video conferencing services, the new collaboration platforms which bring us all here, today.



CroLASA and CPD

2020 - CroLASA introduced the CPD (Continual Professional Development) points on the certificate of attendance

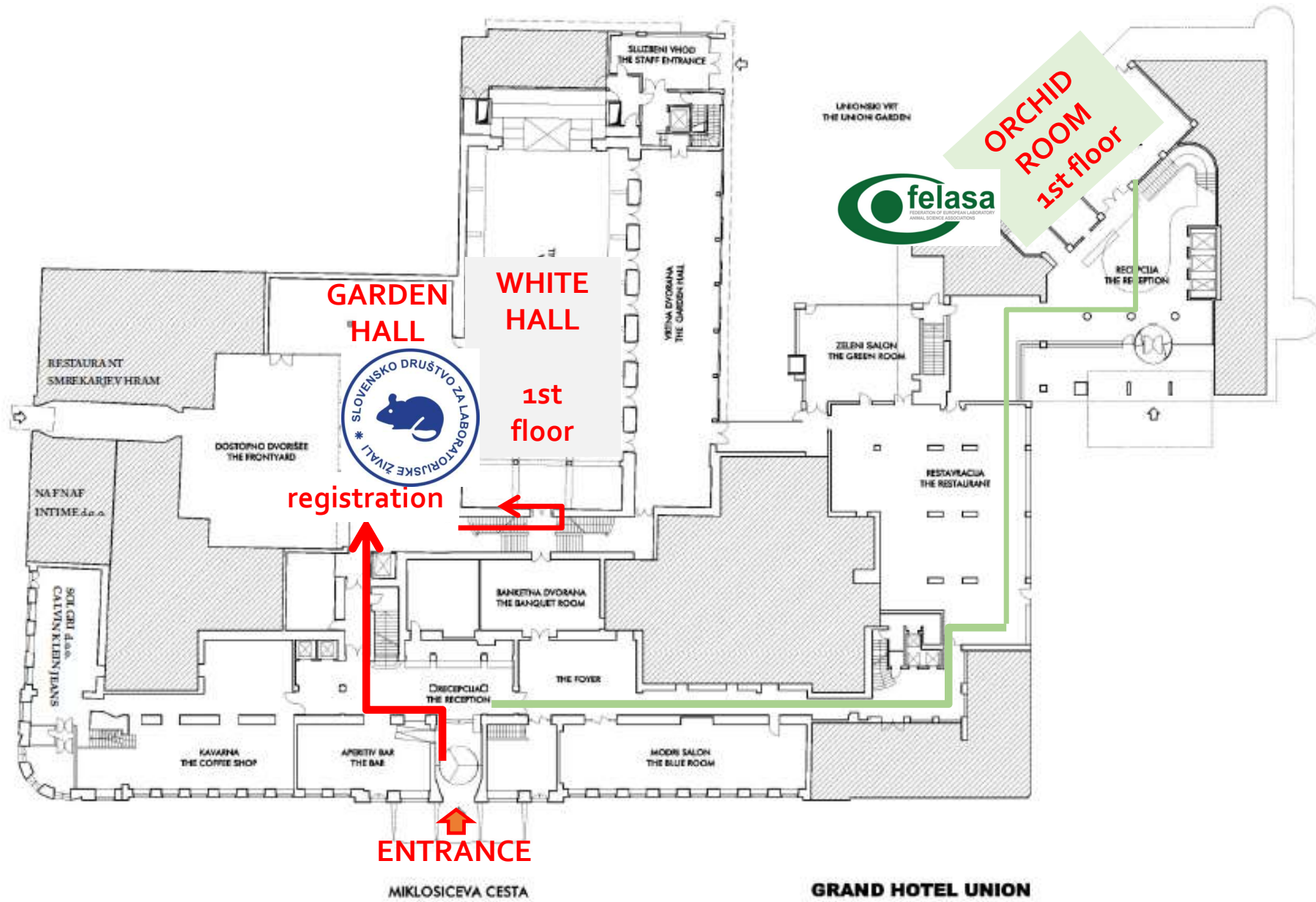
- harmonisation of the national (Croatian) education and training activities with those of other EU member states (e.g. Slovenia and others MS)

- in EU, LAS licence is renewed every 5 years based on the accumulated CPD scores, granted by the course providers and endorsed by the National Competent Authority

June 15	Lectures: White Hall	WS: Orchid room
7.30-8.30	REGISTRATION (Garden Hall)	WS1: 8.00-10.45
8.30-8.50	OPENING: SLAS & CroLASA WELCOME	David Anderson
8.40-8.50	FELASA President: A brief introduction to FELASA	FELASA workshop on classification and reporting of severity of procedures Farm Animal Models
8.50-9.20	L1. Klas Abelson: Refinement of painful procedures – are we good enough?	
9.20-9.50	L2. Delphine Bouard: Improving aseptic conditions in laboratory animals: a major refinement tool	
9.50-10.20	L3. Belen Pintado: Genetically altered animals through the lens of Directive 2010/63/EU	
10.20-10.40	Simon Koren: Reducing animal usage and revealing new insights: the power of <i>in vivo</i> imaging technologies in preclinical research	
10.40 -11.15	COFFEE BREAK	WS3: 11.00-13.30
11.15-11.45	L4. Adrian Smith: PREPARE for Better Science: Guidelines for animal research and testing	Belen Pintado Workshop on specific provisions of Directive 2010/63/EU on the use of genetically altered animals in scientific research
11.45-12.10	L5. Aleš Belič: Animal models: RNA expression analyses as an important source of irreproducibility and low translatability	
12.10-12.25	Anemari Horvat: Stress promotes lipid droplet accumulation in astrocytes (SL1)	
12.25-12.40	Sara Orehek: Antitumor immunity boosted by gasdermin D induced necrosis (SL2)	
12.40-12.55	Polona Kovačič: Extent of necrosis as a measure of acute pancreatitis severity in studies employing live cell imaging (SL3)	
12.55-13.05	Carlo Demalde: Tecniplast – your partner for animal facility	
13.05 -14.15	LUNCH	WS2: 13.45-16.45

13.05 -14.15	LUNCH	WS2: 13.45-16.45
14.15-14.40	L6. Chris Van Ginneken: Pigs in research, what about the piglet?	David Anderson Dolores Bonaparte FELASA workshop on classification and reporting of severity of procedures Rodent & Rabbit Models
14.40-15.05	L7. Alenka Seliškar: Anaesthesia and analgesia in calves, goats, sheep and pigs used for biomedical research	
15.05-15.30	L8. Amir Rosner: Equine species in research and education	
15.30-15.45	Malan Štrbenc: Successful rehoming as ultimate refinement for golden hamsters in SARS-CoV-2 vaccine research (SL4)	
15.45-16.00	Maša Čater: Improving biomedical research by automated behaviour monitoring in the animal home cage (SL5)	
16.00-16.10	Monika Savarin: Labena – Complete solutions in Laboratory and Process Analytics	
16.10-16.45	COFFEE BREAK	
16.45-17.15	L9. Jean-Philippe Mocho: FELASA recommendations for health monitoring and euthanasia of laboratory fish	
17.15-17.20	180s: MR1. Manca Pečjak Pal	
17.20-17.25	180s: MR2. Tajda Gredar	
17.25-17.30	180s: MR3. Sara Trnski	
17.30-17.35	180s: MR4. Dominika Peskar	
17.35-17.40	180s: MR5. Katja Uršič Valentinuzzi	
17.40-17.45	180s: MR6. Sanita Maleškič Kapo	
17.45-17.50	180s: MR7. Maša Čater	
17.50-18.00	Kristijan Jurkovac: Animalab - your trusted partner in life-science research	
18.00-18.30	CHEESE AND WINE RECEPTION	
18.30h	SLAS AWARDS (the best 180s presentations)	

NAZORJEVA ULICA



GRAND HOTEL UNION
PRITLICE / GROUND FLOOR

SPONSORS

5th Congress of the SLAS and 3rd joint SLAS - CroLASA meeting

omegac

 Sanolabor

 **TECNIPLAST**
innovation through passion

mikro**polo**
VAŠ PARTNER ZA LABORATORIJ

 Labena

ANIMA **LAB**


FeliVet



Welcome

5th Congress of the SLAS and 3rd joint SLAS - CroLASA meeting

Improving nonclinical research practices: the way forward

SLAS Executive Committee

SLAS
President
2012-2025



Martina Perše

SLAS
Secretary
2012-2025



Tatjana Pirman

SLAS
Treasurer
2015-2025



Simona Kranjc
Brezar

SLAS
VicePresident
2021-2025



Duško Lainšček

SLAS EC Board members 2021-2025



Malan Štrbenc



Maša Skelin
Klemen



Katja Skulj